

Doping effects of Dy and Mg on BaTiO₃ ceramics prepared by hydrothermal method

Hongyan Miao · Min Dong · Guoqiang Tan · Yongping Pu

© Springer Science + Business Media, LLC 2006

Abstract Fine Dy and Mg-doped barium titanate powders were prepared by hydrothermal method at 240°C with BaCl₂·2H₂O, TiCl₄ and NaOH as the main reactants, Dy₂O₃ and MgCl₂·6H₂O as additives respectively. The substitution style, microstructure and electrical properties of the two kinds of samples were comparatively studied by X-ray diffractometer (XRD), atomic emission spectrum (AES) and scanning electron microscopy (SEM) characterizations. It is confirmed that Dy or Mg enters into the BaTiO₃ lattice. Ba site is replaced if a little Dy₂O₃ is doped but some more Dy will take up the positions of Ti. Mg always substitutes for Ti site. Dy and Mg are both useful to obtain the microstructure with small grains and high density, and the former results in a better microstructure. Dy has no influence on shifting and depressing Curie peak. When Dy₂O₃ content is 0.6 wt%, the dielectric constant rises up to 4250. However, Mg has evident effect on shifting Curie peak. The value of ΔT_c is -40°C in the doping range of 0 to 0.15 wt%. When Mg/Ti atomic ratio is 0.06 in the precursors, the dielectric constant rises up to 4100.

Keywords Barium titanate · Hydrothermal · Dy · Mg

1 Introduction

Barium titanate (BaTiO₃) is the best-known perovskite material and has been broadly used as the raw material for ceramic condensers, memory, and multi-layer ceramic capacitors.

At present, hydrothermal synthesis is considered as one of the best methods used to prepare monodisperse nanometer BaTiO₃ powders, which presents the following major advantages: narrow particle size distribution, low coagulation, high purity and fine crystallization of powders, little pollution during the preparation process, short preparation time and low cost [1, 2].

The soft mode of BaTiO₃ is Slater mode (= stretching vibration between Ti and O₆ octahedra), and the defects on Ba and Ti site can affect the soft mode significantly [3]. For this purpose, the addition of Dy, which is a kind of rare earth elements, and Mg, whose ionic radius (0.065 nm) is similar to that of Ti⁴⁺ [4, 5], into hydrothermal BaTiO₃ particles were chosen to modify the ceramic properties. Moreover, we discussed doping effects of Dy and Mg on BaTiO₃ ceramics through XRD, SEM and AES analysis.

2 Experimental procedure

2.1 Samples preparation

BaCl₂·2H₂O and TiCl₄ were used as precursors, and NaOH was used as mineralizer. All the chemical reagents used were of analytical grade. Initially, TiCl₄ was slowly added to icy water to prepare 0.6 M TiCl₄ aqueous solution. Subsequently, TiCl₄ solution was slowly added into BaCl₂ aqueous solution with continuously stirring. The atomic ratio of Ba/Ti was kept at 2.0. Then, MgCl₂·6H₂O and Dy₂O₃ were added as the sources of magnesium and dysprosium, respectively. The excess NaOH concentration was fixed at 2 M. At last, the mixed precursor solution was sealed in a 50 ml Teflon-lined autoclave with a filling capacity of 60% and soaked at 220–260°C for 10–16 h. After the reaction, the autoclave was cooled naturally to room temperature. The

H. Miao (✉) · M. Dong · G. Tan · Y. Pu
School of Material Science and Engineering,
Shaanxi University of Science and Technology,
Xianyang 712081, People's Republic of China
email: mhy@sust.edu.cn

powders were washed by distilled water until no Cl^- was detected by AgNO_3 . The powders were dried at 90°C and then ball-milled for 4 h before use. Samples in $\Phi 14\text{ mm} \times 2\text{ mm}$ were prepared by dry press and then were sintered at 1275°C for 2 h. At last, silver electrodes were prepared on the BaTiO_3 ceramics samples for dielectric properties measurements.

2.2 Characterizations

The phase and lattice parameters of the powders were determined by a Rigaku D/max-rA roating X-ray diffractometer (XRD). The analysis was performed at 40 kV and 60 mA with Ni-filtered $\text{Cu-K}\alpha$ radiation. The compositions of the BaTiO_3 powders were analyzed by a JY-38plus atomic emission spectrum (AES). The morphologies of BaTiO_3 powders as well as BaTiO_3 ceramics were observed by a PHILIPS XL20 scanning electron microscopy (SEM). Dielectric constant was measured by a Taiwan HE2612 capacitor meter with a test frequency of 1 kHz. The breakdown electric field was measured by an alternating breakdown device.

3 Results and discussion

According to the theory of crystal chemistry, in an ideal perovskite, the ionic radius, r_i ($i = \text{A}, \text{B}, \text{O}$), satisfies the equation: $(r_A + r_O) = \sqrt{2}(r_B + r_O)$ [6]. The Goldschmidt tolerance factor for perovskites is, hence, defined by

$$t = (r_A + r_O) / \sqrt{2}(r_B + r_O) \quad (1)$$

r_A , r_B and r_O respectively represent the radii of A, B position and oxygen ion in the ABO_3 structure. The tolerance factor of Dy^{3+} is 0.87 in A site and 0.89 in B site. Due to their similarity, Dy can replace A and B positions in a certain proportion.

Figure 1 shows the effect of Dy_2O_3 dopant on the lattice parameters of the Dy_2O_3 - BaTiO_3 powders. The lattice parameters were calculated from miller indexes obtained by

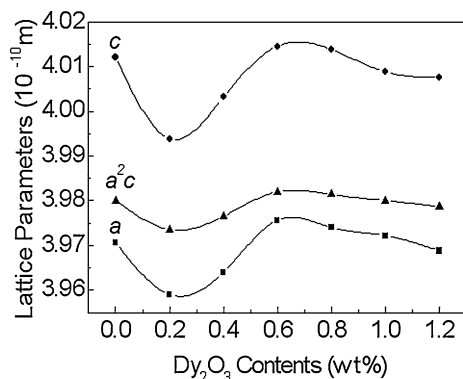
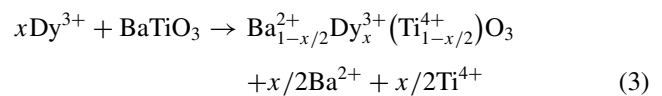
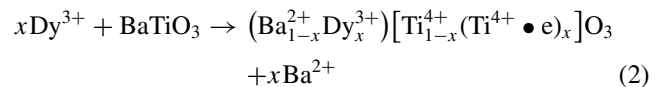


Fig. 1 The dependence of lattice parameters on Dy_2O_3 contents

XRD patterns data. When small amount of Dy_2O_3 was doped, the lattice cell parameters decreased sharply, which indicated that Ba was replaced by Dy because ionic radius of Dy^{3+} is smaller than Ba^{2+} ($= 1.61\text{ \AA}$). However, with increasing amount of the Dy_2O_3 dopant, the values of a and c increased gradually and then leveled off. It indicated that some Dy ions also occupied the positions of Ti because ionic radius of Dy^{3+} is larger than Ti^{4+} ($= 0.68\text{ \AA}$). When the amount of Dy_2O_3 dopant increased to 0.6 wt%, the lattice parameters of the Dy_2O_3 - BaTiO_3 reached the maximum. The above cases conformed the following substituting mechanism (2) and (3) respectively:



The judging method of lattice parameters is unreliable to Mg dopant because its radius (0.065 nm) is similar to that of Ti^{4+} (0.068 nm). In order to confirm whether Mg entered really into the BaTiO_3 lattice or existed as the secondary phase besides BaTiO_3 , XRD measurement of the powders was performed. Figure 2 is XRD patterns of MgO - BaTiO_3 powders with various Mg/Ti atomic ratios. From XRD results, most as-prepared hydrothermal particles were assigned to BaTiO_3 phase and there was only a slight extra diffraction peak belonging to BaCO_3 , which indicated that the Mg dopant did not form other new phases such as MgO , MgCl_2 or MgTiO_3 in doping concentration range of our experiments. Table 1 shows each weight percentage of Ba, Ti and Mg measured using AES analysis. In Table 1, the percentage of Ti decreased with increasing weight percentage of Mg. The above results revealed a fact that Mg did not exist as the secondary phase besides BaTiO_3 in the particles, but existed substitutionally in Ti site of a BaTiO_3 lattice.

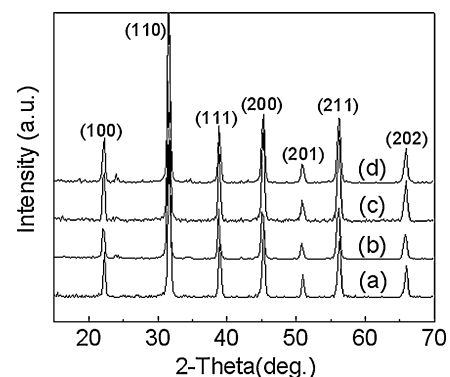


Fig. 2 XRD patterns of MgO - BaTiO_3 powders with various Mg/Ti atomic ratios (240°C) Mg/Ti: (a) 0.06 (b) 0.08 (c) 0.10 (d) 0.15

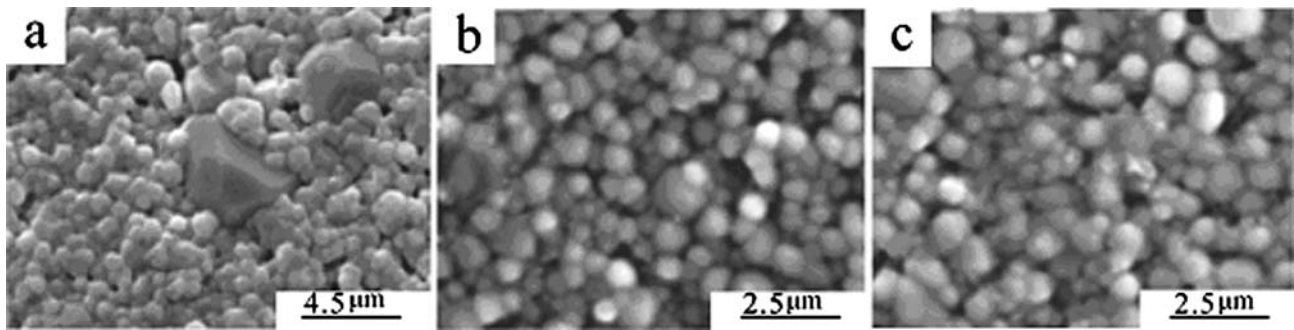


Fig. 3 SEM micrographs of (a) BaTiO₃, (b) Dy₂O₃-BaTiO₃ and (c) MgO-BaTiO₃ ceramics sintered at 1275°C

Figure 3 shows the micrographs of the (a) BaTiO₃, (b) Dy₂O₃-BaTiO₃ and (c) MgO-BaTiO₃ ceramics. From Fig. 3(a), the pure BaTiO₃ ceramics was not uniform in grain size distribution and some large grains were observed, which can affect electric properties of BaTiO₃ ceramics strongly [7–9]. With doping of additives, the grains became smaller, the density became higher, and the cracks and pores accumulation gradually disappeared. Figure 3(b) and (c) are micrographs of BaTiO₃ ceramic surface including Dy and Mg respectively in optimized doping conditions. In Fig. 3(b), Dy₂O₃ content was 0.6 wt%. Grains were well distributed in size of 480 nm and had no abnormal growth. In Fig. 3(c), the best doping condition was 0.06 at Mg/Ti atomic ratio. The surface appearance of (b) was better than that of (c), in which

grain size was about 500 nm. Furthermore, MgO-BaTiO₃ ceramics exhibited a little non-uniform size distribution with slight abnormal growth of grains. We can get a conclusion that Dy₂O₃, compared MgO, is a more excellent kind of growth-constraining agents, which make ceramic materials have microstructure with small grains.

Figure 4 is the curve of dielectric constant versus temperature of Dy₂O₃-BaTiO₃ ceramics sintered at 1275°C, which expresses the effects of Dy content on ceramic electric properties. From the curve, we can believe that in the doping range of Dy, doped ceramics' dielectric character was similar to the pure BaTiO₃ and Curie temperature changed little. It meant that Dy had no evident function on shifting and depressing Curie peak. When Dy₂O₃ content was 0.6 wt%, the dielectric constant rose to 4250 at room temperature.

From dielectric characteristics of BaTiO₃ ceramics including various Mg in Fig. 5, with increasing of the Mg/Ti atomic ratio, the shift of the peaks to lower temperature was observed. The Curie temperature T_c of the MgO-BaTiO₃ ceramics was about 80°C but that of pure BaTiO₃ ceramics was 120°C. The value of ΔT_c was -40°C in the doping range of 0 to 0.15 wt%, and the substitution content of Mg

Table 1 Each percentage by weight of Ba, Ti and Mg

No.	Mg/Ti	Ba (wt%)	Ti (wt%)	Mg (wt%)
1	0	53.3	20.9	0
2	0.02	52.4	22.8	0.0545
3	0.06	52.2	18.7	0.1144
4	0.08	53.5	18.2	0.1304
5	0.10	52.8	17.9	0.1412

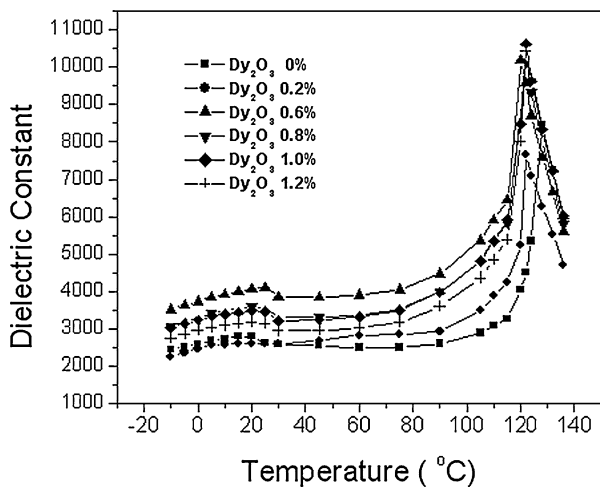


Fig. 4 The curve of dielectric constant vs. temperature of Dy₂O₃-BaTiO₃ ceramics sintered at 1275°C

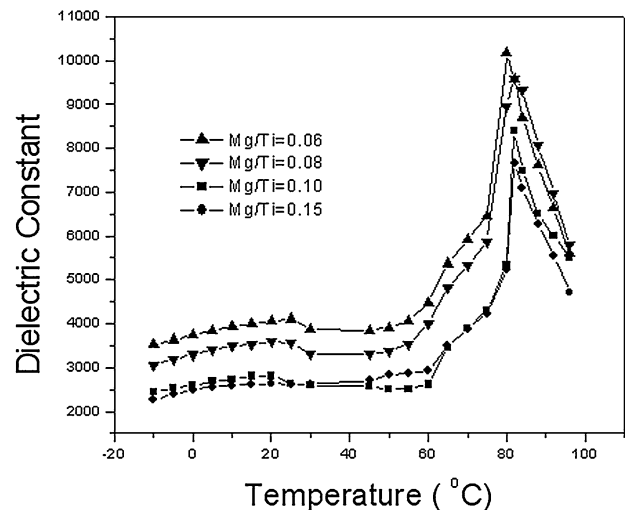


Fig. 5 The curve of dielectric constant vs. temperature of MgO-BaTiO₃ ceramics sintered at 1275°C

in BaTiO₃ solid solution reached the saturated state when referring to a higher content. When Mg/Ti atomic ratio was 0.06, MgO-BaTiO₃ ceramics specimen performed a higher dielectric constant of 4100 at room temperature. It was also indicated that the excess Mg could also depress peak value of dielectric constant sometimes.

From Figs. 4 and 5, we can calculate that when Dy₂O₃ content was 0.6 wt% or Mg/Ti atomic ratio was 0.06, dielectric constant was the most stable and changed between –10% and 10% at a temperature range of –15 – 100°C. Besides these, our test results also show that, without any sintering aids, the breakdown electric field of BaTiO₃ ceramics including Mg and Dy were up to 3.2 kV/mm and 3.0 kV/mm respectively. Compared the value of 2.6 kV/mm for pure BaTiO₃ ceramics, the significant rise of breakdown electric field was due to the obtained small-grain microstructure by doping Dy or Mg.

4 Conclusions

Barium titanate powders including various Dy and Mg were prepared by hydrothermal method at 240°C with BaCl₂·2H₂O, TiCl₄ and NaOH as the main reactants, Dy₂O₃ and MgCl₂·6H₂O as dopants respectively. In our experiment conditions, Dy or Mg entered into the BaTiO₃ lattice. Ba site was replaced if a little Dy₂O₃ was doped. But when the Dy₂O₃ content increased, some Dy ions would take up the positions of Ti. Mg substituted for Ti site all the time because of its similar ionic radius to Ti⁴⁺. Dy and Mg were both useful to constrain the growth of the grains and obtain the microstructure with small grains and high density, and

Dy₂O₃-BaTiO₃ exhibited a better microstructure. Dy₂O₃ had no evident influence on shifting and depressing Curie peak. When Dy₂O₃ content was 0.6 wt%, the dielectric constant rose up to 4250. However, Mg had evident function on shifting Curie peak, and the Curie temperature shifted to lower temperature of 80°C. When Mg/Ti atomic ratio was 0.06, the dielectric constant was up to 4100. In the above two cases, dielectric constants were both much stable and its variation range was ±10% at –15–100°C. The microstructure with small grains and high-density, obtained by doping Dy and Mg, caused breakdown electric field to rise up to 3.2 kV/mm and 3.0 kV/mm respectively without any sintering aids.

Acknowledgment This work was supported by the National Nature Science Foundation of China (NSFC No. 50372039).

References

1. S. Feng and H. Xu, *Acc. Chem. Res.*, **34**(4), 239 (2001).
2. K. Byrappa and Y. Masahiro, *Handbook of Hydrothermal Technology* (William Andrew, New York, 2001), p. 104.
3. S. Wada, M. Yano, T. Suzuki, and T. Noma, *J. Mater. Sci.*, **35**(9), 3889 (2000).
4. H. Kishi, Y. Okino, and M. Honda, *Jpn. J. Appl. Phys.*, **36**(7), 5954 (1997).
5. T. Nagai, K. Iijima, and H.J. Hwang, *J. Am. Ceram. Soc.*, **83**(9), 107 (2000).
6. Y. Tsur, T. Dunbar, and C.A. Randall, *J. Electroceram.*, **28**(7), 25 (2001).
7. P. Hansen, D. Hennings, and H. Schreinemacher, *J. Am. Ceram. Soc.*, **81**(5), 1369 (1998).
8. R. Waser, T. Baiatu, and K.H. Hardtl, *J. Am. Ceram. Soc.*, **73**(6), 1654 (1990).
9. D. Hennings and H. Schreinemacher, *J. Eur. Ceram. Soc.*, **15**(11), 795 (1995).